



Aerosol–Cloud–Rainfall Properties Inferred from Satellite Observations Over Different Regions of the Indian Subcontinent: Variability, Trends and Relationships During the Summer Monsoon

P. P. LEENA,¹ N. SRAVANTHI,^{1,2} V. ANIL KUMAR,¹ G. PANDITHURAI,¹ and A. S. PANICKER¹

Abstract—In the present work, the variability, trends and relationships of aerosol, cloud and rainfall are explored for three regions of the Indian subcontinent: the Indo-Gangetic Plain (IGP), central India (CI) and the North Indian Ocean (NIO). The investigated properties include the monthly averages of satellite retrievals for the aerosol optical depth (AOD), angstrom exponent (AE), aerosol index (AI), cloud effective radius (R_c), cloud optical thickness (COT), cloud liquid water path (LWP) and rain rate (RR). Inter-annual and seasonal variability and long-term trends for these properties were analyzed over the regions selected. The analysis showed apparent regional and temporal variations in all seven parameters. Strong increases in aerosol properties over the IGP and CI regions over the last two decades have enabled the study of the response to cloud and rainfall properties. Further, aerosol–cloud–rain rate relationships during the summer monsoon were verified using linear fit analysis (using AOD [and AI], R_c , LWP and RR) for the three regions, respectively. A negative relation between AOD and R_c was seen over the three regions, whereas AOD and RR showed a negative relation over IGP and NIO. It was found that the AI property, which represents the aerosol number, is inversely correlated with R_c but positively correlated with RR during the monsoon season over the IGP and CI. AI and LWP showed a negative relation for CI but a positive relation for IGP and NIO. We believe that this study will help in assessing regional and global climate impacts due to aerosols.

Keywords: Aerosol–cloud–rainfall properties, variability, trends, Indian subcontinent, satellite observations.

1. Introduction

Atmospheric aerosols influence climate directly by scattering and absorbing shortwave radiation

(Haywood & Boucher, 2000), and indirectly by influencing the formation of clouds (Albrecht, 1989; Lohmann & Feichter, 2005; Twomey, 1974, 1977). An increase in aerosol number concentration with constant liquid water content leads to an increase in cloud droplet number concentration (CDNC) and a decrease in droplet size, followed by an increase in cloud optical thickness (COT) and albedo (Twomey, 1974). These aerosol particles can modify/alter the cloud and rainfall characteristics by (i) increasing the cloud droplet and ice particle concentrations, hence impacting the optical properties of different phases of warm, ice and mixed cloud formation (Boucher et al., 2013; Liu et al., 2012; Yuan et al., 2008), and (ii) decreasing the precipitation efficiency of warm clouds and thus altering the cloud lifetime and albedo, consequently altering the indirect radiative forcing (Sorooshian et al., 2010). All these effects/processes can contribute to aerosol–cloud–precipitation interactions; hence in-depth study of their properties is required to obtain a better scientific understanding.

Levin and Cotton (2009) described the difficulties in establishing a relationship between aerosols and precipitation and determining the indication of a change in the latter due to aerosols in climatology. This complexity is possibly caused by the multifarious interactions between environmental and meteorological parameters, radiation, aerosols and cloud microphysics and its dynamics. A few studies (e.g., Andreae et al., 2004; Jones & Christopher, 2010) have observed a relation between aerosols and cloud properties. Satellite observations have shown that the cloud albedo effect due to aerosols is about $-0.2 \pm 0.1 \text{ W m}^{-2}$ (Quaas et al., 2008), and the

¹ Indian Institute of Tropical Meteorology, Ministry of Earth Sciences, Dr. Homi Bhabha Road, Pashan, Pune 411008, India. E-mail: leena@tropmet.res.in

² State Key Laboratory of Tropical Oceanography, South China Sea Institute of Oceanology, Guangzhou, China.

value is much lower than the estimates from chemical transport or global climate model simulations (median value of -0.7 W m^{-2} with a 5–95% range of -0.3 to -1.8 W m^{-2}) mentioned in the Intergovernmental Panel on Climate Change (IPCC) reports (Forster et al., 2007). Satellite observations have shown modifications in cloud characteristics due to aerosols (Kaufman & Fraser, 1997) and even from the biomass burning in the Amazon Basin (Johnson et al., 2004). Studies have also been carried out to verify the relationship between aerosol and cloud properties (Nakajima et al., 2001; Wetzal & Stowe, 1999). Other studies (Jones & Christopher, 2010; Peng et al., 2002) have observed a positive correlation between the aerosol optical depth and cloud effective radius for regions like the Arabian Sea and the Amazon Basin, respectively.

The Indian subcontinent is densely populated and industrialized, a source region for aerosols, a land-mass with coastal areas, inland plains and mountains, and even experiencing different climate conditions, which demands aerosol–cloud–precipitation–related studies. A few studies have been conducted over different regions of the Indian land mass, Bay of Bengal, Arabian Sea and Indian Ocean to study the linkages between aerosol–cloud–rainfall properties, in particular using satellite observations (e.g. Ramachandran & Kedia, 2013; Tripathi et al., 2007). The reported results have shown that aerosol

distribution, sources and removal processes vary on a regional scale. These studies have shown that (i) among the existing measurements, satellite observations are a potential tool if we compensate for the resolution, and (ii) more information on aerosol–cloud–rainfall properties and their relationship will prove useful in assessing regional and global climate impacts due to aerosols.

2. Data Used

In the present study, 16 years (March 2000 to December 2015) of aerosol optical depth (AOD), angstrom exponent (AE), Aerosol Index (AI), cloud effective radius (R_e), cloud optical thickness (COT), cloud liquid water path (LWP) and rain rate (RR, which is also termed rainfall) data are used. Table 1 summarizes the data used for the present analysis. All the above-mentioned parameters are organized into four seasons throughout the analysis. Seasons are taken as monsoon (June–July–August–September or JJAS), post-monsoon (October–November, or ON), winter (December–January–February, or DJF) and pre-monsoon (March–April–May, or MAM). The details are discussed below.

Table 1

Summary of the observations used for the present study

Parameters	Details	References
AOD	AOD _{550nm} 01° × 01°	http://giovanni.gsfc.nasa.gov/
AE	Deep blue AE for land and AE_1 and_2_ocean 01° × 01°	https://ladsweb.modaps.eosdis.nasa.gov/ https://atmosphere-imager.gsfc.nasa.gov/products/aerosol/
AI	AOD × AE 01° × 01°	
COT	COT _{liquid} 01° × 01°	http://giovanni.gsfc.nasa.gov/
R_e	$R_{e \text{ liquid}}$ 01° × 01°	http://giovanni.gsfc.nasa.gov/
LWP	Derived from R_e and COT 01° × 01°	
RR	TMPA 3B42 3-hourly data 0.25° × 0.25°	http://giovanni.gsfc.nasa.gov/

2.1. Aerosol and Cloud Products

The aerosol properties were analyzed using AOD_{550nm} and AE, and similarly, the cloud optical properties were analyzed using R_e and COT. AOD is the measure of aerosols distributed within the column of air from the top of the atmosphere to the earth's surface, and AE provides information on the typical aerosol particle size. Higher AE (e.g. > 1.2) indicates that smaller sub-micrometer-sized aerosols dominate the AOD, while smaller AE (e.g. < 0.5) indicates AOD dominance of larger super-micrometer-sized aerosols. The aerosol number concentration is particularly important for aerosol interactions with clouds and precipitation. This aerosol property is much better (than AOD) represented by the Aerosol Index (AI), which is the product of AOD and AE, because aerosol concentrations are dominated by sub-micrometer aerosol sizes. COT is the vertical optical thickness between the top and bottom of a cloud. R_e is the weighted mean of the size distribution of cloud droplets.

All the above-mentioned aerosol and cloud properties are obtained from the MODIS (Moderate Resolution Imaging Spectroradiometer) Terra satellite. MODIS Terra (with a 10:30 IST equatorial crossing time) views the earth's entire surface every 1–2 days, acquiring data in 36 spectral bands ranging in wavelength from 0.4 to 14.4 μm . Validation of aerosol products against the ground-based Aerosol Robotic Network (AERONET) data showed (i) a correlation coefficient of about 0.5–0.7 over the Indian landmass (Ichoku et al., 2002; Prasad & Singh, 2007), and (ii) about 68% of the ocean retrievals matched the AERONET data to within $0.03 \pm 10\%$ (Patadid et al., 2017). In addition, the quality of the MODIS AOD retrievals decreased when the underlying surface became heterogeneous and/or bright, such as deserts and urban regions (Gupta et al., 2013; Levy et al., 2010). For the present study, monthly data with a spatial resolution of $01^\circ \times 01^\circ$ were used. For cloud retrievals, data from overcast pixels were used (broken scenes lead to R_e overestimates). It should be noted that both COT and R_e refer to the lower-altitude (water) clouds and are retrieved

together using bi-spectral methods (e.g. Nakajima & King, 1990). More information on data can be obtained from <http://giovanni.gsfc.nasa.gov/> or <https://ladsweb.modaps.eosdis.nasa.gov/>. Further, using cloud optical properties, the cloud liquid water path (LWP) was estimated using the equation given below. LWP is a measure of the weight of the liquid water droplets in the atmosphere above a unit surface area on the earth, and the relation is

$$\text{LWP} = \frac{2}{3} \cdot \rho_w \cdot R_e \cdot \text{COT},$$

where ρ_w is liquid water density.

2.2. Rainfall Product

In the present work, monthly RR calculated from the 3-hourly rainfall data is used. The Tropical Rainfall Measuring Mission (TRMM), a joint space mission between NASA and the Japan Aerospace Exploration Agency (JAXA), was designed to monitor and study tropical rainfall. TRMM uses five instruments (<https://climatedataguide.ucar.edu/>): Precipitation radar (PR), TRMM Microwave Imager (TMI), Visible Infrared Scanner (VIRS), Clouds and Earths Radiant Energy System (CERES) and Lightning Imaging Sensor (LSI). The TMI and PR are the main instruments used for precipitation. The TRMM Multi-satellite Precipitation Analysis (TMPA) provides monthly precipitation averages (TMPA 3B43) and daily and sub-daily (3-hourly) averages (c 3B42), which are probably the most relevant TRMM-related products for climate research. TMPA 3B42 and 3B43 are available in 0.25° spatial resolution, covering 50°N to 50°S . Reports (Prakash et al., 2015, 2016) have shown that TMPA-V7 (version 7) data sets represent the mean seasonal rainfall characteristics reasonably well, but they show an overestimation of rainfall over most parts of the country except over the orographic regions. According to the reports, TMPA 3B42-V7 is closer to the India Meteorological Department (IMD) gauge-based observations, possibly due to gauge adjustments (Prakash et al., 2015, 2016). More information on data can be obtained from <http://giovanni.gsfc.nasa.gov/>.

3. Aerosol–Cloud–Rain Rate Distribution over the Indian Subcontinent and Objectives

In this section, a general study is carried out to determine the aerosol, cloud and rain rate distribution over the Indian subcontinent. The climatological patterns of AOD, COT and RR for MAM, JJAS, ON and DJF are shown in Fig. 1. In general, all three parameters showed apparent spatiotemporal variability. AOD (first row of Fig. 1) values over the Indian Ocean and Bay of Bengal were low irrespective of the season. With the exception of JJAS, AOD was consistently smaller over the Arabian Sea. The southwestern and central regions of India showed higher AOD values during JJAS, which is mainly due to the dust aerosols. AOD was also higher over the Indo-Gangetic Plain, irrespective of the season, and was comparatively higher during JJAS. The western and eastern regions of India showed higher AOD during MAM and JJAS, with values higher than 0.4. Higher AOD over the northern region of the Indian subcontinent may be attributed to the industries and

urban centers, and thus enhanced anthropogenic activity compared to southern peninsular India. In other words, the growth of industrialization and automobile transportation along with the continuous increase in population has led to increased AOD values, especially over the northern region (Kumar, 2014). It can even be noted that dust aerosols also contribute to AOD distribution during JJAS (Dey et al., 2004; Manoj et al., 2011) as well as MAM. Long-range transport of dust from Arabia or arid regions during pre-monsoon result in high AOD especially over the western and eastern regions of India.

COT (second row of Fig. 1) values over the Indian Ocean varied from 5 to 10 irrespective of the season, whereas in the Bay of Bengal, they were quite low during MAM and DJF. With the exception of JJAS, COT was consistently smaller over the Arabian Sea. Over the southern peninsula, COT was higher during JJAS and ON, and it was the highest during JJAS over southwestern India. Over central India, COT showed higher values during JJAS and slightly

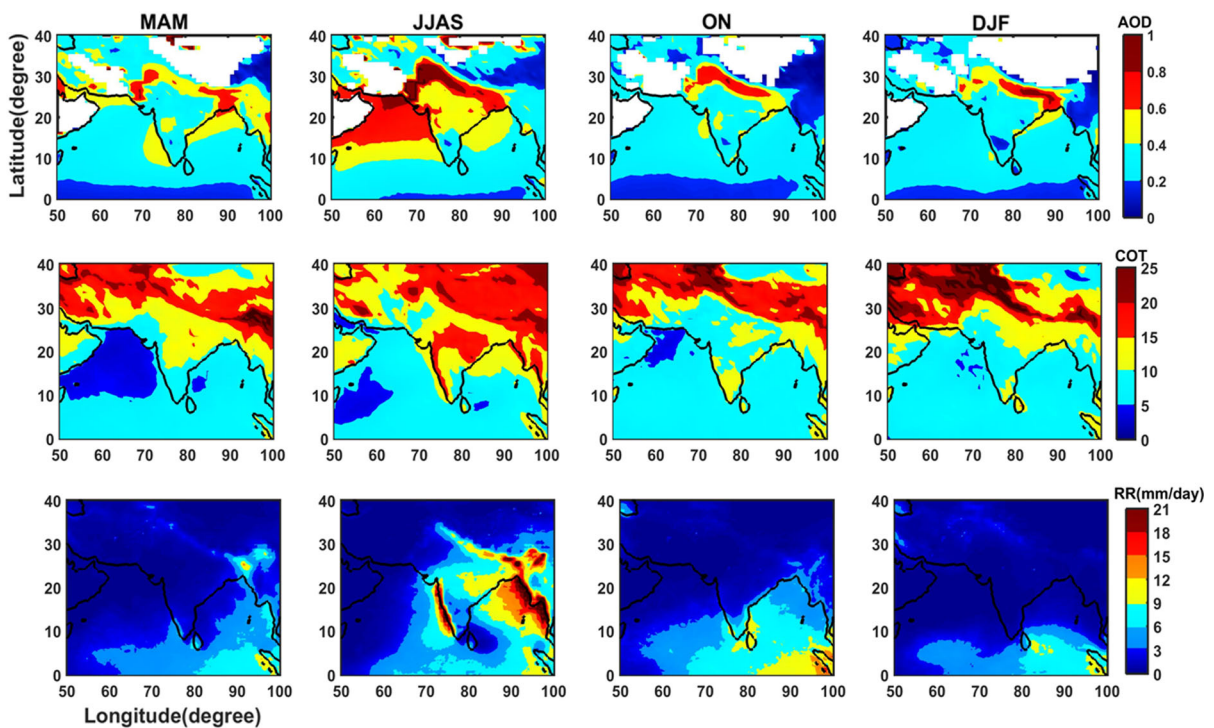


Figure 1
The climatological pattern of AOD, COT and RR for MAM, JJAS, ON and DJF, respectively

lower values during MAM. Over northern India and the Indo-Gangetic Plain, COT was higher irrespective of the season. This variability was similar over the eastern region of India. The western part of the Indian subcontinent showed COT values ranging from 5 to 10 during JJAS but less than 5 for the other seasons. RR (third row of Fig. 1) over the Indian Ocean and Bay of Bengal was slightly higher during JJAS and ON compared to MAM and DJF. Over the Arabian Sea, with the exception of JJAS, all seasons showed RR less than 5—in other words, rainfall activity was absent. Over the landmass, rainfall activity was higher (greater than 10 mm/day) over the southwest, central and northeastern parts of India during JJAS. Southern peninsular India showed wet conditions during MAM, JJAS and ON. The southeastern region of India showed rainfall activity during JJAS and ON, respectively. Overall analysis showed (i) a distinct spatiotemporal distribution of aerosol, cloud and rainfall properties over the Indian subcontinent, and (ii) an apparent latitudinal variability in these variables. Additionally, the topography of the Indian subcontinent (Fig. 2) showed that the landmass includes mountain, coastal and plateau regions, which can give rise to local convection, acting as a barrier to the free flow of air, especially at lower levels.

Considering all the above, in the present work we focus on (i) analyzing the temporal variation and trends in aerosol–cloud–rain rate properties, and (ii) investigating the aerosol–cloud–rainfall relationship

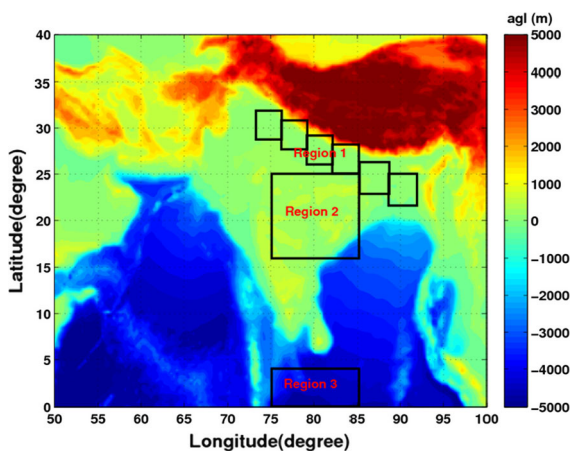


Figure 2

Topography of Indian subcontinent with study region highlighted in solid boxes

during the summer monsoon using statistical analysis. To fulfill these objectives, we have selected three regions, i.e. the Indo-Gangetic Plain (IGP), central India (CI) and the North Indian Ocean (NIO) (highlighted in Fig. 2). Details of the regions are as follows:

- i. Region 1: IGP region, which has been taken as combining six sectors (boxes from left to right in Fig. 2e), i.e. 1 (73° E– 76° E, 29° N– 32° N), 2 (76° E– 79° E, 28° N– 31° N), 3 (79° E– 82° E, 26° N– 29° N), 4 (82° E– 85° E, 25° N– 28° N), 5 (85° E– 88° E, 23° N– 26° N) and 6 (88° E– 92° E, 22° N– 25° N)
- ii. Region 2: (75° E– 85° E, 16° N– 25° N) as CI
- iii. Region 3: (75° E– 85° E, 0° N– 4° N) as NIO

It should be noted that throughout this paper, the parameters mentioned in Sect. 2 are averaged over the above-mentioned grids and represented in four seasons.

These regions were selected because they are highly important with respect to aerosol loading and their potential role in modulating monsoon behavior. All three regions are covered with both scattering and absorbing types of aerosols, among which the IGP is highly polluted in terms of the absorbing type of aerosols. Further, we know that the Indian summer monsoon has a great impact on water resource management, agriculture and food production (Manoj et al., 2012). Manoj et al. (2011) noted that the monsoonal winds are greatly influenced by the tropospheric temperature gradient between CI and the NIO. The aerosol-rich CI and part of the IGP and the pristine environment of the IO create a meridional temperature gradient which leads to a large amount of moisture convergence towards CI, creating a condition conducive for large-scale organized convection over the CI region (Manoj et al., 2011). It is also noted that the maximum value of AOD is seen over the IGP region (Ravi Kiran et al., 2009), and it is interesting to observe that the maximum loading of aerosols during break monsoon conditions is located north of but parallel to the climatological position of the monsoon trough (Manoj et al., 2011). This action leads to modulation of monsoon circulation (Manoj et al., 2011, 2012).

4. Results

4.1. Temporal Variation in Aerosol, Cloud and Rain Rate Properties

In this section, the inter-annual, monthly and seasonal variation in aerosol, cloud and rain rate properties and annual trends are discussed using seven parameters i.e., AOD, AE, AI, R_e , COT, LWP and RR, for three study regions.

4.1.1 Inter-annual Variation

The inter-annual variability in AOD, AE, AI, R_e , COT, LWP and RR from 2000 to 2015 over the IGP, CI and NIO regions is shown in Fig. 3. It can be seen that AOD varied broadly from 0.50 to 0.80 over the IGP, 0.30 to 0.45 over CI, and less than 0.20 over the NIO region. AOD values over the IGP region were higher compared to CI and NIO. Over the IGP region, the years 2002, 2004, 2011 and 2015 showed higher AOD values (greater than 0.6). Over CI, AOD

showed little year-to-year variation, but showed an increasing trend overall, with an increase from approximately 0.30 to 0.45. Over the NIO, no significant variation in AOD was noted throughout the study period. AE (Fig. 3b) showed clear inter-annual variations over selected regions, with clearly increasing trends over IGP and CI. IGP showed low AE during 2000 (~ 0.60) and higher AE during 2011 (~ 1.20). Interestingly, over CI and IGP, a sudden increase in AE was observed from 2003 onwards. Over NIO, there was little year-to-year variation in AE. Lower values in AE were noted during 2000 (0.53) and higher values in 2015 (0.83). AI, an aerosol property which represents the aerosol number much better than AOD, displayed strongly increasing trends over IGP and CI—but not for NIO (Fig. 3c). A clear inter-annual variation in AI was noted over the IGP region compared to NIO and CI (Fig. 3c).

R_e (Fig. 3d) did not show any significant inter-annual variation for any of the three regions, but overall values over IGP and CI ($\sim 14 \mu\text{m}$) were

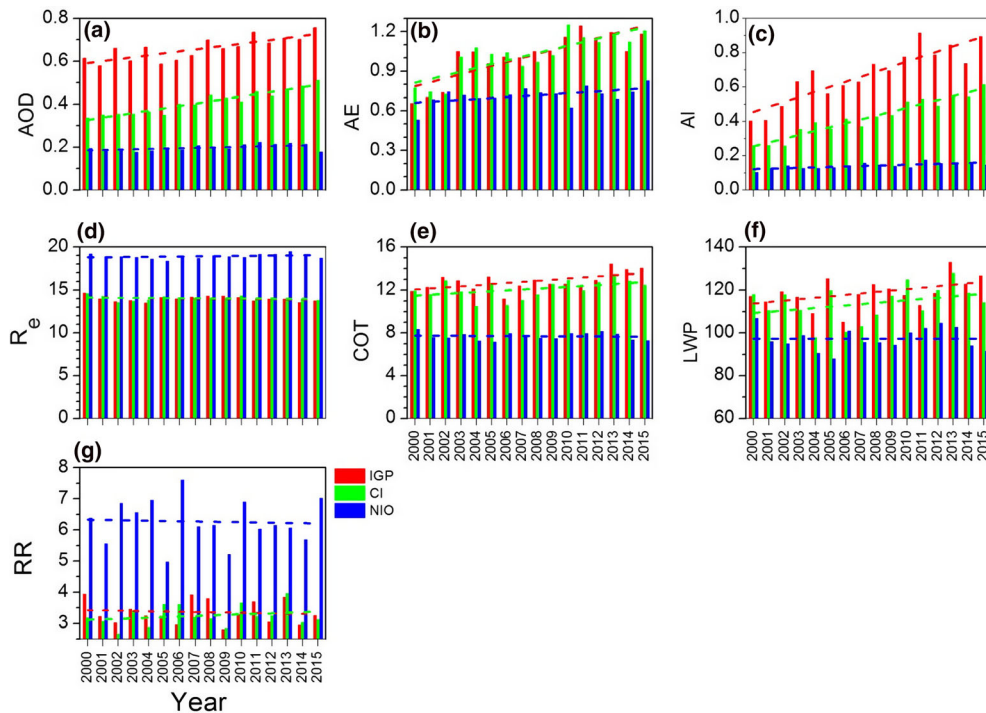


Figure 3

Inter-annual variations in **a** AOD, **b** AE, **c** AI, **d** R_e , **e** COT, **f** LWP and **g** RR from 2000 to 2015 for the three study regions. Line represents the linear trend line

lower than for NIO ($\sim 19 \mu\text{m}$). Higher values over oceanic regions compared to continental regions may be broken cloud fields, as frequently found over oceans, leading to R_e overestimates. COT (Fig. 3e) showed higher values over IGP and CI compared to the NIO region. A low COT value was observed in 2006 (~ 11) over IGP and in 2004 (~ 10) over CI. For both regions, higher COT values were observed during 2013. Very low COT (less than 7) was observed over NIO throughout the study period. LWP (Fig. 3f) varied from 100 to 130 g m^{-2} over IGP, 95 to 130 g m^{-2} over CI, and 85 to 110 g m^{-2} over the NIO region. A lower value of LWP (105 g m^{-2}) was recorded in 2006 and a higher value (130 g m^{-2}) in 2013 over the IGP region. Over CI, a low LWP value (99 g m^{-2}) was observed in 2004 and a high value ($\sim 130 \text{g m}^{-2}$) in 2013. A lower value of LWP (89 g m^{-2}) was observed in 2005 and a higher value (109 g m^{-2}) in 2000 for the NIO region. A distinct inter-annual variation in RR was observed irrespective of the region. A high RR value was observed in 2007 (2013) over the IGP (CI). Similarly, a higher value of RR (7.76 mm/day) was observed in 2006 over the NIO region.

Next, the trend in the annual mean of all seven parameters was investigated for the three regions using linear trend analysis. The trend analysis and slope values (along with percentage change in trend) are presented in Fig. 3 and Table 2. In general, AOD, AE and AI showed an increasing trend over IGP and CI. Over NIO, no trend was found in AOD, AE or AI. R_e showed a decreasing (increasing) trend over IGP and CI (NIO). COT and LWP showed an increasing

trend over IGP and CI. Over NIO, a decreasing trend in COT was observed, but no trend was found in LWP. Rainfall showed a negative trend over IGP and NIO but a positive trend over CI. Overall, the analysis showed (i) regional variability in the annual mean trend in aerosol, cloud and rainfall properties, and (ii) strong aerosol variability over IGP and CI from which changes to cloud and precipitation properties were expected, and increasing or decreasing trends in all parameters may be due to the seasonal variation in the respective variables.

4.1.2 Monthly and Seasonal Variation

First, the monthly variation in AOD, AE, AI, R_e , COT, LWP and RR over the IGP, CI and NIO (figure not shown) were analyzed. In general, AOD was low over NIO and higher over IGP, irrespective of month. It was observed that all three regions exhibited higher AOD during May to September. Over IGP, there was a decreasing trend in AOD from January to April, and from May onwards there was an increasing trend, reaching a maximum during July and then decreasing again. Overall, the same pattern was observed over CI, with higher AOD during the month of July. AOD over NIO was quite low irrespective of month. AE showed clear monthly variation and a similar pattern over IGP and CI, with a clearly increasing trend from April to September. A high value of AE was observed in January and September over IGP, whereas over CI, a higher value was seen in the month of September. Over NIO, a very high value of AE was recorded in March and November. Monthly variations in AI showed similar patterns over IGP and CI, with higher values over IGP in January and higher values over CI from July to September. AI was higher during March and November over NIO. R_e showed similar variations over IGP and CI, whereas the values over NIO were higher than $18 \mu\text{m}$ irrespective of month. Higher R_e was observed during July to September and lower values during January and December over IGP. CI showed high R_e from July to September. Over NIO, lower values of R_e were observed from January to March, and a peak in June. COT showed clear monthly variation over IGP and CI as compared to NIO. In IGP, COT was higher in the months of January, June

Table 2

Slope values obtained from linear trend lines for three regions, respectively. Bracket value represents the percentage change in the trend

Parameters	IGP	CI	NIO
AOD	0.01 (23)	0.01 (52)	0.00 (−8)
AE	0.03 (80)	0.03 (56)	0.01 (55)
AI	0.03 (121)	0.02 (137)	0.00 (42)
R_e (μm)	−0.02 (−6)	−0.01 (−5)	0.02 (−2)
COT	0.10 (17)	0.08 (4)	−0.01 (−12)
LWP (g m^{-2})	0.67 (8)	0.60 (−3)	0.00 (−14)
RR (mm day^{-1})	−0.01 (−17)	0.02 (−2)	−0.01 (9)

and December, and quite low during November. COT showed high values during July and August over CI. Irrespective of month, the NIO region showed a very low COT value. LWP showed almost the same value range over IGP and CI, with higher values in the month of July. Over NIO, LWP showed quite low month-to-month variation. Both IGP and CI followed the same pattern in RR, with the highest during July and August. Over NIO, during April and November the RR was higher than in other months.

Next, the seasonal variation in AOD, AE, AI, R_e , COT, LWP and RR for the three regions was analyzed and is presented in Fig. 4. IGP showed higher AOD during JJAS and less during MAM, ON and DJF. CI also showed higher AOD during JJAS, and for the other three seasons showed almost the same values. AOD values observed over NIO were quite low irrespective of season, with slightly higher values in JJAS. Seasonal variability in AE (Fig. 4b) showed higher values during DJF and lower values during MAM over IGP. CI showed high AE during ON and lower AE during MAM. Over NIO, AE was very low during JJAS, and all other seasons showed a similar variation. AI (Fig. 4c) was higher during DJF

over IGP and during JJAS over CI, and no significant seasonal variation was seen over the NIO region. Higher aerosol (lower AE values) contribution over IGP and also over CI during JJAS was likely due to more dust transported from Arabia across the oceans. Manoj et al. (2011) observed much larger transport and accumulation of desert dust aerosols due to associated closed-circulation anomalies during breaks followed by active monsoon cases. During winter and post-monsoon, the aerosol contribution over the IGP and CI may be from biomass burning or forest fires, which accumulate due to the shallow boundary layer and calm winds (Ramachandran et al., 2020). On comparing all three regions, AOD showed higher values (low AE values mean on average larger aerosol particles) during MAM and JJAS over IGP, indicating the possibility of long-range transport of dust over the area.

The seasonal variability in R_e (Fig. 4d) over IGP and CI exhibited comparatively higher values during JJAS and ON. During these seasons, the convective activity is stronger, leading to more precipitating clouds and thus higher R_e . Over NIO, irrespective of season, R_e varied from 15 to 20 μm , and it was higher

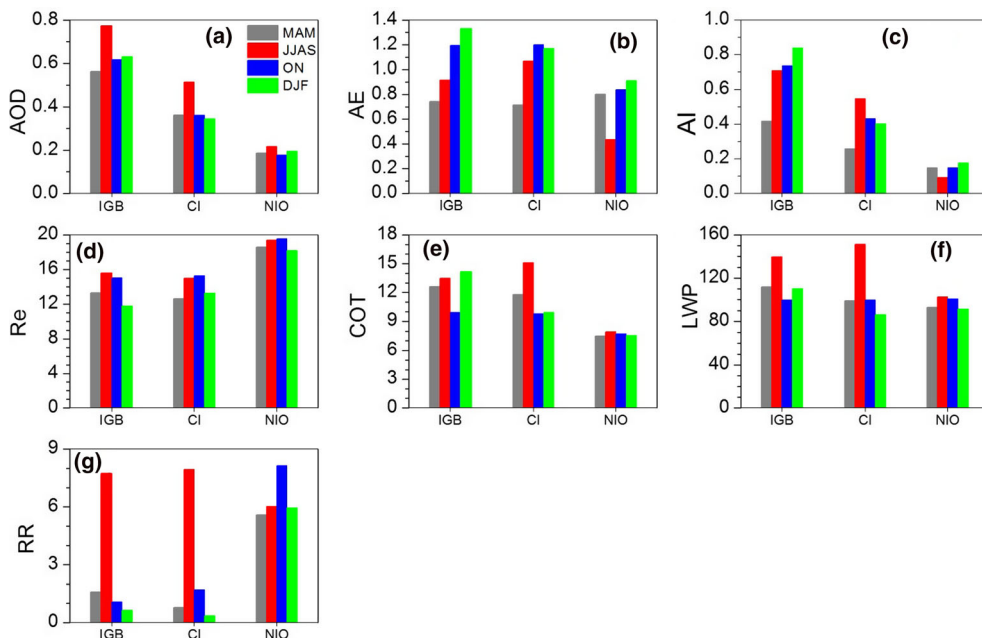


Figure 4

Bar plot showing seasonal variation in a AOD, b AE, c AI, d R_e , e COT, f LWP and g RR for the three study regions

than over the IGP and CI regions. COT (Fig. 4e) showed higher values (greater than 12) during JJAS and DJF over IGP, whereas it was higher over CI only in JJAS. Lower COT values were observed during ON for both IGP and CI. In addition, for CI, COT during ON and DJF showed similar values, with a negligible difference. Over IGP and CI, the LWP (Fig. 4f) was higher during JJAS than during the other three seasons. Over NIO, seasonal variability in LWP was quite low, with a value less than 100 g m^{-2} , irrespective of season. RR showed a prominent peak during JJAS over IGP and CI, whereas the peak was in ON for NIO. In general, these aerosol characteristics can in turn modulate the cloud properties and even affect the precipitation efficiency.

4.2. Aerosol–Cloud–Rainfall Relationship During Summer Monsoon and Related Discussion

In this section, linear fit analysis is used to investigate the relationship between the aerosol–cloud–rain rate during the summer monsoon. The linear fit analysis is carried out between (i) the AOD and cloud properties–rain rate and (ii) the AI (property representing aerosol number concentration) and cloud properties–rain rate. The significance of these relationships is tested using the *t* test. Table 3 shows the correlation coefficient (*r*) obtained from the linear fit analysis between (i) AOD and R_e , (ii) AOD and

LWP, (iii) AOD and R_e (normalized with LWP), (iv) AOD and RR, (v) AI and R_e , (vi) AI and LWP, (vii) AI and R_e (normalized with LWP), and (viii) AI and RR for the three regions. A negative relation between AOD and R_e was observed irrespective of the region, with a higher correlation for CI (-0.62) and lower for NIO (-0.04). AOD and LWP showed a negative relation for IGP and CI, whereas it was positive for NIO. This may be dependent on the cloud type; i.e., with a more stratiform cloud type, the suppression of precipitation with high aerosols can indeed be expected. Linear fit analysis between AOD and R_e normalized with LWP also showed a negative relation, with a higher correlation coefficient for IGP (-0.37). A negative relation was shown between AOD and RR over the IGP and NIO. Further linear fit analysis was performed between AI and cloud properties–rain rate. The analysis showed a negative relation between AI and R_e (or R_e normalized with LWP), irrespective of region. The correlation between AI and LWP showed positive a relation for IGP and NIO and a negative relation for the CI region. The negative relation between aerosol property and R_e agrees well with the aerosol first indirect effect. It is also noted that there is a positive relation between AI and RR over IGP and CI but a negative relation over NIO. This is probably due to (i) more convective cloud systems during JJAS over IGP and CI, more pollution (e.g. higher AI), which initially delays precipitation only, but then via a more intense convection yields higher RR, and (ii) the aerosol indirect effect might even be larger for the aerosol pristine background such as the NIO region. Values that are significant at $p < 0.10$ are highlighted in bold in Table 3.

Table 3

Correlation coefficient value (*r*) obtained from AOD vs. R_e , AOD vs. LWP, AOD vs. ($R_e \times \text{LWP}^{-1/3}$), AOD vs. RR, AI vs. R_e , AI vs. LWP, AI vs. ($R_e \times \text{LWP}^{-1/3}$) and AI vs. RR for three regions respectively (bold value shows significant at $p < 0.10$)

S. no.	Variables	Correlation coefficient (<i>r</i>)		
		IGP	CI	NIO
1	AOD and R_e	-0.47	-0.62	-0.04
2	AOD and LWP	-0.13	-0.46	0.33
3	AOD and ($R_e \times \text{LWP}^{-1/3}$)	-0.37	-0.20	-0.25
4	AOD and RR	-0.08	0.01	-0.45
5	AI and R_e	-0.36	-0.52	-0.42
6	AI and LWP	0.07	-0.30	0.22
7	AI and ($R_e \times \text{LWP}^{-1/3}$)	-0.41	-0.23	-0.39
8	AI and RR	0.27	0.39	-0.48

5. Discussion

For a detailed understanding, the obtained results were compared with earlier studies conducted over different regions of the Indian subcontinent, Arabian Sea, Bay of Bengal and Indian Ocean using satellite observations. A summary of aerosol, cloud and rainfall relationship studies (including data used, study region, study period, etc.) carried out using satellite observations is provided in Table 4. It should

Table 4

Summary of the aerosol, cloud and rainfall relationship studies done over the Indian region using satellite observations (especially covering large grid and with correlation analysis)

Study	Region and period	Observation used
Tripathi et al. (2007)	Indo-Gangetic Plain including Thar Desert JJAS (2001–2005)	AOD and CER from MODIS
Manoj et al. (2012)	Central India (CI; 73–82° E; 18–28° N) and peninsular India (PI; 73.5–80.5° E, 7.5–17.5° N) During the break period of monsoon 2009	AOD, CER, CERice, COD, CF, CTP, CLWP, CIP from MODIS satellite
Hazra et al. (2013)	India region (70–90° E, 10–35° N) JJAS (2003–2009)	RR from CMAP AOD, COT, CF, CDER, CIER from MODIS
Ramachandran and Kedia (2013)	Arabian Sea, India and the Bay of Bengal JJAS (2001–2010)	RR from TRMM AOD, CER, COT from MODIS AAI from TOMS and OMI
Gopal et al. (2016)	Southern part of India including urban (Hyderabad, Bangalore), coastal (Visakhapatnam, Trivandrum) and arid regions (Anantpur, Pune) 2005–2014	AOD, CTP and CF from MODIS
Patil et al. (2017)	Region 1: IGP region Region 2: Central India Region 3: Western India JJAS (2000–2009)	Daily mean rainfall data (1° × 1°), provided by the Indian Meteorological Department (IMD) AOD, CDER, CTP from MODIS
Saranghi et al. (2017)	Region (17–27° N, 75–88° E) for broad study and point observation for correlation analysis JJAS (2006–2015) (includes April–May and October for increasing sample)	collocated AOD (from AERONET)–RR (from rain gauge) measurements at hourly temporal resolution over IITK were used to illustrate the association between aerosol–rainfall as a representation
Present study	Region 1: IGP region Region 2: Central India Region 3: North Indian Ocean JJAS (2000–2015)	RR from TRMM AOD, CER from MODIS AI, LWP calculated

be noted that this survey was mainly focused on those studies which considered large area/grid and carried out a linear fit analysis. As can be seen from Table 4, several studies have been carried out specifically over the Indian region to determine the relation among aerosol, cloud and rainfall properties. Among these studies, Tripathi et al. (2007), Patil et al. (2017) and Saranghi et al. (2017) investigated the IGP region, where Saranghi et al. (2017) verified the relation between AOD and rainfall (represented as “RR” hereafter), and the other two investigated the relation between AOD and cloud effective radius (CER) or AOD and cloud top pressure (CTP). Their studies showed a positive relation between aerosol loading and rainfall. Patil et al. (2017) found that the relation with AOD and CER was negative or positive if the rainfall years were categorized as deficient or abundant, respectively. Manoj et al. (2012) and Patil et al. (2017) carried out studies over CI but did not show

any linear fit analysis between AOD and RR. Manoj et al. (2012) showed a negative relation between cloud properties and AOD. Similarly, a positive relation between CTP and AOD was seen irrespective of deficient or abundant rainfall years. Gopal et al. (2016) verified the relation of cloud properties with AOD irrespective of season for six regions in the southern part of India. Overall, the analysis showed a positive (negative) relation between cloud fraction (CF) and AOD (CTP and AOD). Hazra et al. (2013) showed a relation between aerosol, cloud and rainfall properties over the Indian region covering land and ocean. This study reported a negative relationship ($r = -0.07$) between RR and AOD and a positive relationship between RR and cloud properties. Ramachandran and Kedia (2013) verified the relationship of aerosol, cloud and rainfall specifically over the Arabian Sea, Indian landmass and Bay of Bengal. In general, RR and AOD showed a negative

relation irrespective of region. A positive (negative) relation was seen between CER and AOD over the Arabian Sea (Indian landmass and Bay of Bengal). COT showed a negative correlation with AOD irrespective of the region. Overall, the survey showed that most studies have concentrated on the landmass, i.e., over CI, IGP, western India and southern India, and much less on the oceans. A comparison of the linear fit analysis carried out in the present study, i.e., AOD with both R_e and RR, over the IGP region showed that the results of the investigation are in agreement with earlier studies for the same region. The review also showed that, over CI, the monsoon core region, studies were mainly carried out to investigate the aerosol–cloud–rainfall relationship by categorizing the rainfall years/periods, i.e. either during break periods or classifying as deficient or abundant. The correlation coefficient obtained from AOD with R_e over CI from the present study is aligned with the reports of Ramachandran and Kedia (2013); however, as mentioned above, they reported for a larger grid, not for core CI. Interestingly, there are no reports from the Indian Ocean region.

Taken together, this analysis will provide additional information on the relationship of aerosol, cloud and rainfall over the core CI and the Indian Ocean, where studies are sparse. The results, along with the review carried out, suggest that aerosol alone has no effect on the Indian summer monsoon, resulting in a weak relation between aerosol and rainfall (Hazra et al., 2013). Our recent study (Leena et al., 2018) using ground-based and satellite observations from the Western Ghats region on precipitation susceptibility of monsoon clouds to changes in aerosols suggested that precipitation is suppressed at the medium range of the integrated liquid or liquid–water path (i.e. 500–1000 g m⁻²). This may be a reason for the nonsignificant values obtained from the *t* test carried out between AOD and RR. Both positive and negative relations between aerosol–cloud properties and aerosol–rainfall were observed. The positive relation is likely due to the following: (1) lack of complete removal of aerosols by wet deposition; (2) a large spatial gradient of atmospheric heating induced by absorbing types of aerosols which can lead to large-scale moisture flux convergence and low-level uplift for convection

organization, which will enhance moist static instability, leading to convection and to an active condition (Manoj et al., 2011); (3) abundance of fine-mode aerosols despite heavy rainfall (e.g. Leena et al., 2016); and (4) hygroscopic growth of aerosol particles due to an increase in relative humidity (Ramachandran & Kedia, 2013). The negative relation likely reflects the wet removal of aerosol particles due to heavy rainfall or the weak moisture convergence failing to create active rainfall. This happens mostly after a break condition where there is aerosol loading during the break phase.

6. Conclusions

In the present work, aerosol–cloud–rainfall properties and their relationship during summer monsoon were studied over the IGP, CI and NIO using 16 years of satellite observations. The properties of AOD, AE, AI, R_e , COT, LWP and RR obtained/derived from satellite observations were investigated. Inter-annual and seasonal variability in the seven parameters was analyzed specifically over the selected regions, which showed clear spatiotemporal variability from the ocean to the landmass. The main conclusions are summarized below.

- i. Linear trend analysis to annual mean values of all seven parameters showed an increasing trend in aerosols over IGP and CI. This increased pollution adversely affected the cloud microphysical properties and precipitation over this region.
- ii. This study showed a negative relation between AOD (or AI) and R_e irrespective of the areas selected. Analysis between AI and LWP showed a negative relation for CI but a weak positive relation for IGP and NIO.
- iii. Analysis also showed a positive relation between AI and RR over IGP and CI and a negative relation over NIO, suggesting the presence of different cloud regimes during the investigated JJAS season.

Detailed analysis suggested that spatiotemporal variability in aerosol properties can in turn affect clouds and precipitation. We believe that this study will help in assessing regional and global climate

impacts due to aerosols and the need for their regulation in this changing climate scenario.

Acknowledgements

Authors thank the Director, IITM for his full support. Indian Institute of Tropical Meteorology (IITM) is fully funded by the Ministry of Earth Sciences (MoES), Government of India, New Delhi. All the data sources are duly acknowledged.

Publisher's Note Springer Nature remains neutral with regard to jurisdictional claims in published maps and institutional affiliations.

REFERENCES

- Albrecht, B. A. (1989). Aerosols, cloud microphysics, and fractional cloudiness. *Science*, *245*, 1227–1230.
- Andreae, M. O., Rosenfeld, D., Artaxo, P., Costa, A. A., Frank, G. P., Longo, K. M., & Silva-Diass, M. A. F. (2004). Smoking rain clouds over the Amazon. *Science*, *303*, 1337–1342.
- Boucher, O., Randall, D., Artaxo, P., Bretherton, C., Feingold, G., Forster, P., Kerminen, V. M., Kondo, Y., Liao, H., Lohmann, U., Rasch, P., Sathesh, S. K., Sherwood, S., Stevens, B., & Zhang, X. Y. (2013). Clouds and aerosols. In T. F. Stocker, D. Qin, G.-K. Plattner, M. Tignor, S. K. Allen, J. Boschung, A. Nauels, Y. Xia, V. Bex, & P. M. Midgley (Eds.), *Climate change 2013. The physical science basis. Contribution of Working Group I to the Fifth Assessment Report of the Intergovernmental Panel on Climate Change*. Cambridge: Cambridge University Press.
- Dey, S., Tripathi, S. N., Singh, R. P., & Holben, B. N. (2004). Influence of dust storms on aerosol optical properties over the Indo-Gangetic basin. *Journal of Geophysical Research*. <https://doi.org/10.1029/2004JD004924>
- Forster, P., Ramaswamy, V., Artaxo, P., Bernsten, T., Betts, R., Fahey, D., Haywood, J., Lean, J., Lowe, D., Myhre, G., Nganga, J., Prinn, R., Raga, G., Schulz, M., & Van Dorland, R. (2007). *Climate change 2007. The physical science basis. Contribution of Working Group I to the Fourth Assessment Report of the Intergovernmental Panel on Climate Change, chap. Changes in atmospheric constituents and in radiative forcing* (pp. 129–243). Cambridge: Cambridge University Press.
- Gopal, R. K., Raja Obul Reddy, K., Balakrishnaiah, G., Arafath, S. M. D., Siva Kumar Reddy, N., Chakradhar Rao, T., Lokeswara Reddy, T., & Ramakrishna Reddy, R. (2016). Regional trends of aerosol optical depth and their impact on cloud properties over Southern India using MODIS data. *Journal of Atmospheric and Solar Terrestrial Physics*, *146*, 38–48.
- Gupta, P., Khan, M. N., da Silva, A., & Patadia, F. (2013). MODIS aerosol optical depth observations over urban areas in Pakistan: Quantity and quality of the data for air quality monitoring. *Atmospheric Pollution Research*, *4*, 43–52.
- Haywood, J., & Boucher, O. (2000). Estimates of the direct and indirect radiative forcing due to tropospheric aerosols. A review. *Review of Geophysics*, *38*, 513–543.
- Hazra, A., Taraphdar, S., Halder, M., Pokhrel, S., Chaudhari, H. S., Salunke, K., & Mukhopadhyay, P. (2013). Indian summer monsoon drought 2009: Role of aerosol and cloud microphysics. *Atmospheric Science Letters*, *14*, 181–186.
- Ichoku, C., Chu, D. A., Mattoo, S., Kaufman, Y. J., Remer, L. A., Tanre, D., Slutsker, I., & Holben, B. N. (2002). A spatio-temporal approach for global validation and analysis of MODIS aerosol products. *Geophysical Research Letters*, *29*(12), Art. No. 1616.
- Johnson, G., Ristovski, Z., & Morawska, L. (2004). Application of the VH-TDMA technique to coastal ambient aerosols. *Geophysical Research Letters*, *31*, L16105. <https://doi.org/10.1029/2004GL020126>
- Jones, T. A., & Christopher, S. A. (2010). Statistical properties of aerosol–cloud–precipitation interactions in South America. *Atmospheric Chemistry and Physics*, *10*(5), 2287–2305. <https://doi.org/10.5194/acp-10-2287-2010>
- Kaufman, Y. J., & Fraser, R. S. (1997). The effect of smoke particles on clouds and climate forcing. *Science*, *277*, 1636–1639.
- Kumar, A. (2014). Long term (2003–2012) spatio-temporal MODIS (Terra/Aqua level 3) derived climatic variations of aerosol optical depth and cloud properties over a semi arid urban tropical region of Northern India. *Atmospheric Environment*. <https://doi.org/10.1016/j.atmosenv.2013.10.030>
- Leena, P. P., Anil Kumar, V., Sravanthi, N., Patil, R., Chakravarty, K., Saha, S. K., & Pandithurai, G. (2018). On the precipitation susceptibility of monsoon clouds to aerosols using high-altitude ground-based observations Western Ghats, India. *Atmospheric Environment*, *185*, 128–136.
- Leena, P. P., Pandithurai, G., Anil Kumar, V., Murugavel, P., Sombawne, S. M., & Dani, K. K. (2016). Seasonal variability in aerosol, CCN and their relationship observed at a high altitude site in Western Ghats. *Meteorology and Atmospheric Physics*. <https://doi.org/10.1007/s00703-015-0406-0>
- Levin, Z., & Cotton, W. R. (2009). *Aerosol Pollution impact on precipitation. A scientific review*. New York: Springer.
- Levy, R. C., Remer, L. A., Kleidman, R. G., Mattoo, S., Ichoku, C., Kahn, R., & Eck, T. F. (2010). Global evaluation of the collection 5 MODIS dark-target aerosol products over land. *Atmospheric Chemistry and Physics*, *10*(2010), 10399–10420.
- Liu, X., Shi, X., Zhang, K., Jensen, E. J., Gettelman, A., Barahona, D., Nenes, A., & Lawson, P. (2012). Sensitivity studies of dust ice nuclei effect on cirrus clouds with the Community Atmosphere Model CAM5. *Atmospheric Chemistry and Physics*, *12*, 12061–12079. <https://doi.org/10.5194/acp-12-12061-2012>
- Lohmann, U., & Feichter, J. (2005). Global indirect aerosol effects. A review. *Atmospheric Chemistry and Physics*, *5*, 715–737.
- Manoj, M. G., Devara, P. C. S., Joseph, S., & Sahai, A. K. (2012). Aerosol indirect effect during the aberrant Indian Summer Monsoon breaks of 2009. *Atmospheric Environment*, *60*, 153–163.
- Manoj, M. G., Devara, P. C. S., Safai, P. D., & Goswami, B. N. (2011). Absorbing aerosols facilitate transition of Indian monsoon breaks to active spells. *Climate Dynamics*, *37*, 2181–2198. <https://doi.org/10.1007/s00382-010-0971-3>
- Nakajima, T., Higurashi, A., Kawamoto, K., & Penner, J. E. (2001). A possible correlation between satellite-derived cloud

- and aerosol microphysical parameters. *Geophysical Research Letters*, 28, 1171–1174.
- Nakajima, T., & King, M. D. (1990). Determination of the optical thickness and effective particle radius of clouds from reflected solar radiation measurements. Part I: Theory. *Journal of Atmospheric Sciences*, 47, 1878–1893. [https://doi.org/10.1175/1520-0469\(1990\)0472.0.co;2](https://doi.org/10.1175/1520-0469(1990)0472.0.co;2)
- Patadid, F., Levy, R. C., & Mattoo, S. (2017). The uncertainty in MODIS aerosol optical depth retrievals in the vicinity of clouds. American Geophysical Union, Fall Meeting 2017, abstract #A51G-2155
- Patil, N., Dave, P., & Venkataraman, C. (2017). Contrasting influences of aerosols on cloud properties during deficient and abundant monsoon years. *Scientific Report*, 7, 44996. <https://doi.org/10.1038/srep44996>
- Peng, Y., Lohmann, U., Leaitch, R., Banic, C., & Couture, M. (2002). The cloud albedo–cloud droplet effective radius relationship for clean and polluted clouds from RACE and FIRE.ACE. *Journal of Geophysical Research*. <https://doi.org/10.1029/2000JD000281>
- Prakash, S., Ashis, K. M., Imranali, M. M., Pai, D. S., Rajagopal, E. N., & Basu, S. (2015). Comparison of TMPA-3B42 versions 6 and 7 precipitation products with gauge-based data over India for the southwest monsoon period. *Journal of Hydrometeorology*. <https://doi.org/10.1175/JHM-D-14-0024.1>
- Prakash, S., Ashis, K. M., Rajagopal, E. N., & Pai, D. S. (2016). Assessment of TRMM-based TMPA-3B42 and GSMaP precipitation products over India for the peak southwest monsoon season. *International Journal of Climatology*, 36, 1614–1631. <https://doi.org/10.1002/joc.4446>
- Prasad, A. K., & Singh, R. P. (2007). Comparison of MISR–MODIS aerosol optical depth over the Indo-Gangetic basin during the winter and summer seasons (2000–2005). *Remote Sensing of Environment*, 107, 109–119. <https://doi.org/10.1016/j.rse.2006.09.026>
- Quaas, J., Boucher, O., Bellouin, N., & Kinne, S. (2008). Satellite-based estimate of the direct and indirect aerosol climate forcing. *Journal of Geophysical Research*, 113, D05204. <https://doi.org/10.1029/2007JD008962>
- Ramachandran, S., & Kedia, S. (2013). Aerosol–precipitation interactions over India. Review and future perspectives. *Advances in Meteorology*. <https://doi.org/10.1155/2013/649156>
- Ramachandran, S., Rupakhetib, M., & Lawrence, M. G. (2020). Black carbon dominates the aerosol absorption over the Indo-Gangetic Plain and the Himalayan foothills. *Environment International*, 142, 105814. <https://doi.org/10.1016/j.envint.2020.105814>
- Ravi Kiran, V., Rajeevan, M., Vijaya Bhaskara Rao, S., & Prabhakara Rao, N. (2009). Analysis of variations of cloud and aerosol properties associated with active and break spells of Indian summer monsoon using MODIS data. *Geophysical Research Letters*, 36, L09706. <https://doi.org/10.1029/2008GL037135>
- Sarang, C., Tripathi, S. N., Kanawade, V. P., Koren, I., & Pai, D. S. (2017). Investigation of the aerosol–cloud–rainfall association over the Indian summer monsoon region. *Atmospheric Chemistry and Physics*, 17, 5185–5204.
- Sorooshian, A., Feingold, G., Lebsock, M. D., Jiang, H., & Stephens, G. L. (2010). Deconstructing the precipitation susceptibility construct. Improving methodology for aerosol–cloud precipitation studies. *Journal of Geophysical Research*, 115, D17201. <https://doi.org/10.1029/2009JD013426>
- Tripathi, S. N., Pattnaik, A., & Dey, S. (2007). Aerosol indirect effect over Indo-Gangetic plain. *Atmospheric Environment*, 41, 7037–7047.
- Twomey, S. (1974). Pollution and the planetary albedo. *Atmospheric Environment*, 8, 1251–1256.
- Twomey, S. (1977). The influence of pollution on the shortwave albedo of clouds. *Journal of Atmospheric Sciences*, 34, 1149–1152.
- Wetzel, M. A., & Stowe, L. L. (1999). Satellite-observed patterns in stratus microphysics, aerosol optical thickness, and shortwave radiative forcing. *Journal of Geophysical Research*, 104(31), 287–299.
- Yuan, T., Li, Z., Zhang, R., & Fan, J. (2008). Increase of cloud droplet size with aerosol optical depth: An observation and modeling study. *Journal of Geophysical Research*. <https://doi.org/10.1029/2007jd008632>